CSN 94-334

How and Why Wonder Book of CLEO Tracking Conventions

Rob Kutschke

September 1, 1996

Abstract

This note summarizes some of the conventions used by the CLEO tracking code, particularly sign conventions. It also contains descriptions of assorted trivia one needs in order to communicate with members of the CLEO tracking group. Finally, the bibliography contains a list of useful CBX and CSN notes from the past few years.

1 The CLEO Coordinate System

The righthanded coordinate system used in the CLEO tracking code has,

- $\hat{x}$ South, outside of ring.
- $\hat{y}$ Up.
- $\hat{z}$ West, this is the positron direction.

2 Track Parameters

The CLEO II helical track parameters are, in `DRIVER` language,

`CUCD` the signed curvature ($= q/2\rho$), where ρ is the radius of curvature and where q is the electric charge, in units of the proton charge.

`FICD` the azimuth of $\mathbf{p}$, measured at the point of closest approach of the track to the z-axis. Here $\mathbf{p}$ is the momentum vector of the track.

`DACD` the signed 2-D distance of closest approach of the track to the z-axis. The sign convention is described in section 6.

`CTCD` the cotangent of the polar angle (tangent of the dip angle).

`ZOCD` the value of z at the point of closest approach of the track to the z-axis.

In this note these five quantities will be denoted by, κ, ϕ_0, d_0, $\cot\theta$ and z_0. Also, quantities appearing in `typewriter` font denote names of programs, subroutines, common blocks, variables etc.

The point of closest approach of the track of the track to the z-axis is traditionally referred to as the point of closest approach to the origin (PCAO). Here the word "origin" refers to the origin in the r-ϕ plane and it is implicit that one is referring to the projection of the track onto this plane. Similarly, d_0 is usually referred to as the distance of closest approach to the origin (DCAO).

Other quantities which will be used in this note are:

- ρ the radius of curvature, $= 1/(2|\kappa|)$. In this note ρ is unsigned.
- $\mathbf{d_0}$ the 2-vector from the origin to the PCAO. Note that d_0 is not the magnitude of $\mathbf{d_0}$; it is a signed quantity (see section 6).
- $\mathbf{p}$ the momentum vector at an arbitrary point along the track.
- p the magnitude of $\mathbf{p}$.
- ϕ the azimuth of $\mathbf{p}$ at some point along the track.
- $\mathbf{p}_0$ the momentum vector at the PCAO.
- p_0 the magnitude of $\mathbf{p}_0$.
- ψ the turning angle from the PCAO to some point on the track. Regardless of charge, this is positive when moving from the PCAO outward along the track.
- s the sagitta of the measured arc of a track.
- S the arc length from the PCAO to some point on the track.
- $S_\perp$ the projection of S onto the x-y plane.
- $\mathbf{p}_\perp$ the projection of $\mathbf{p}$ onto the r-ϕ plane.
- $p_\perp$ the magnitude of $\mathbf{p}_\perp$.
- $\mathbf{B}$ the magnetic field vector.
- B the magnitude of $\mathbf{B}$.
- d_f the signed distance of closest approach of a track to a wire, computed from track parameters and wire positions.
- d_m the signed distance of closest approach of a track to a wire, computed from the measured TDC value.
- (x_c, y_c) the coordinates, in the z=0 plane, of the center of curvature.

Unless otherwise specified, the units of these quantities follow the convention: lengths (m), angles (radians), energies (GeV) and magnetic field (T). This is true both within this note and in the code.

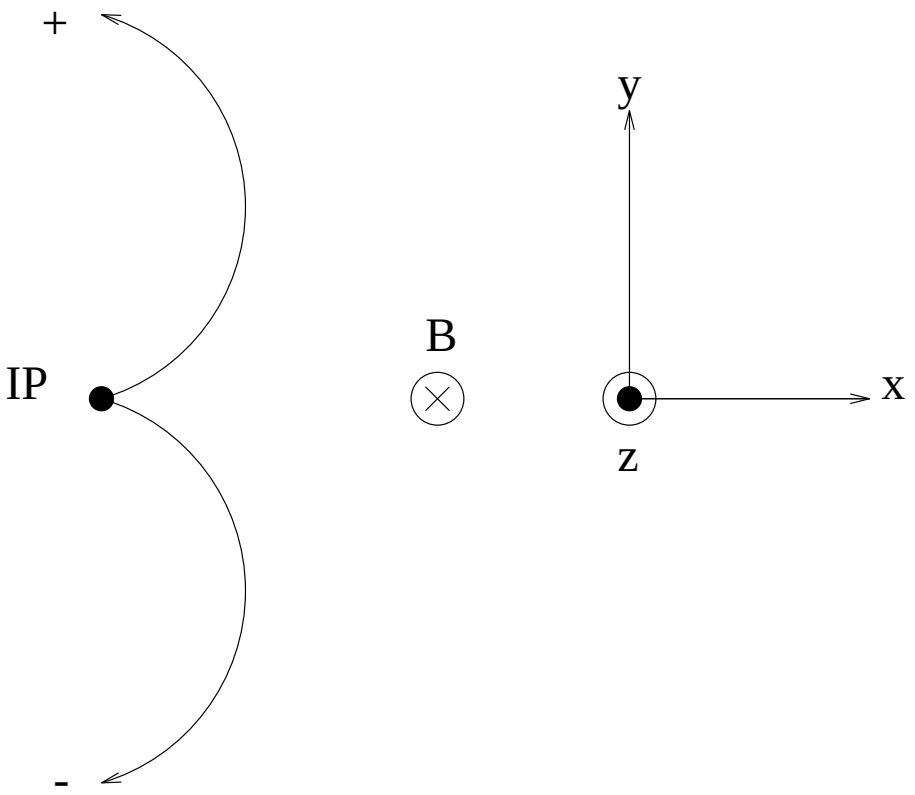

Figure 1: The sign convention for positively and negatively charged tracks.

3 B and the Sign of the Curvature

The CLEO tracking code assumes that the magnetic field is homogeneous throughout the entire tracking volume and that it is exactly aligned with the $-\hat{\mathbf{z}}$ axis (East). The sign of the curvature is simply the electric charge of the track (it is also the sign of $d\phi/dS$). Figure 1, which is drawn with the magnetic field ($\mathbf{B}$) pointing into the page, shows two tracks coming from the interaction point (IP). The track which curves counterclockwise has positive curvature and the one which curves clockwise has negative curvature. The axes of the coordinate system are shown in the right hand part of the figure and the direction of the magnetic field is shown in the middle of the figure. This view is the same as is used by the display program `cleoxd`.

With $\mathbf{B}$ in the negative z direction, a point on a track, and the momentum vector at that point, are expressed, in terms of the turning angle, ψ, as follows,

$$x = x_c + q\rho\sin(\phi_0 + q\psi) \qquad y = y_c - q\rho\cos(\phi_0 + q\psi) \qquad z = z_0 + \rho\psi\cos\theta$$

$$p_x = p_\perp\cos(\phi_0 + q\psi) \qquad p_y = p_\perp\sin(\phi_0 + q\psi) \qquad p_z = p_\perp\cot\theta.$$

For $\mathbf{B}$ in the positive z direction, the correct expression is found by substituting $q \to -q$.

4 Relations between ρ and κ

The relationship between transverse momentum, the magnetic field and the radius of curvature is,

$$p_\perp = (c \times 10^{-9}) q B \rho, \tag{1}$$

where the units are, $p_\perp$(GeV/c), B(T), ρ(m), $c(m/s)$ and where the charge is in units of the charge of the proton. For a particle of unit charge moving in a field of $B = 1.5$ T this gives,

$$p_\perp = 0.4496886\, \rho.$$

The magnitude of the momentum is then,

$$p = 0.4496886\, \rho \sqrt{1 + \cot^2 \theta}.$$

In CLEO the curvature is defined by,

$$\kappa = \frac{q}{2\rho}.$$

It has units of m^{-1}. When comparing to other conventions for helix parameters there are two things of which to be wary. Firstly, most of the standard literature uses $\kappa = q/\rho$. Secondly, a small fraction of the literature considers κ to be an unsigned quantity. With the CLEO definition for κ, the momentum is expressed as,

$$p = \frac{0.2248443}{|\kappa|} \sqrt{1 + \cot^2 \theta}.$$

5 Sagitta

Figure 2 should be interpreted as the projection onto the r-ϕ plane of the helical trajectory of a track which starts from the IP, enters a chamber at point A and exits the chamber at point C. The trajectory within the chamber is the arc ABC. The center of curvature of the circle is the point O, the radius of curvature is ρ, and the point D bisects the chord AC. The sagitta, s, of the arc AC is the line segment BD. For a typical track, the chord AC corresponds to a line running approximately radially outward from the innermost layer of the PT to the outermost measurement on the track. If the track traverses the full DR then $|AC| \simeq 0.85$ m. If the track curls inside the maximum radius of the DR, then the sagitta is equal to ρ (CLEO does not include hits from the inward branch of a curling track). A little trigonometry gives,

$$s = \rho - \sqrt{\rho^2 - \frac{|AC|^2}{4}}.$$

The values of ρ, κ and s for various values of $p_\perp$ are given in Table 1.

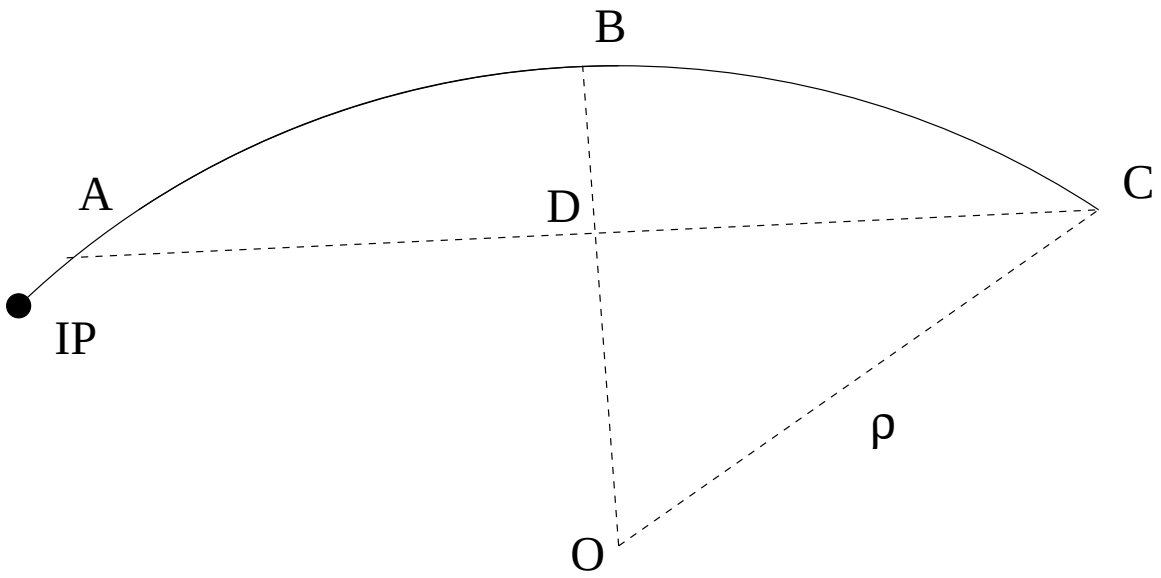

Figure 2: Figure for explanations about the sagitta.

$p_\perp$	ρ	$\lvert\kappa\rvert$	s
(GeV)	(m)	(m^{-1})	(m)
0.100	0.22	2.25	0.222
0.225	0.50	1.00	0.236
0.450	1.00	0.50	0.095
1.000	2.22	0.22	0.041
2.500	5.56	0.09	0.016
5.000	11.12	0.04	0.008

Table 1: Values of ρ, κ and the sagitta as a function of $p_\perp$.

6 Sign Convention for d_0

The track parameter d_0 is defined as the signed 2-D distance of closest approach of the track to the z axis. The sign convention of d_0 is given as follows: first complete the circle which is the projection of the helical track onto the r-ϕ plane. If the origin lies outside of this circle then d_0 and κ have the same sign. Four possible cases are illustrated in Figure 3. In each of the parts of this figure, the solid circle marks the origin and the open circle marks the PCAO. The arc of each track is shown by the solid line and the arrow shows the direction of the particle. The dashed line shows the magnitude of d_0 and the neighbouring $+$ or $-$ sign gives the sign of d_0. The orientation of the coordinate system is shown in the bottom right hand corner of the figure: the z axis comes out of the page but the magnetic field goes into the page.

With the above definitions, one can define the (signed) radius of the center of

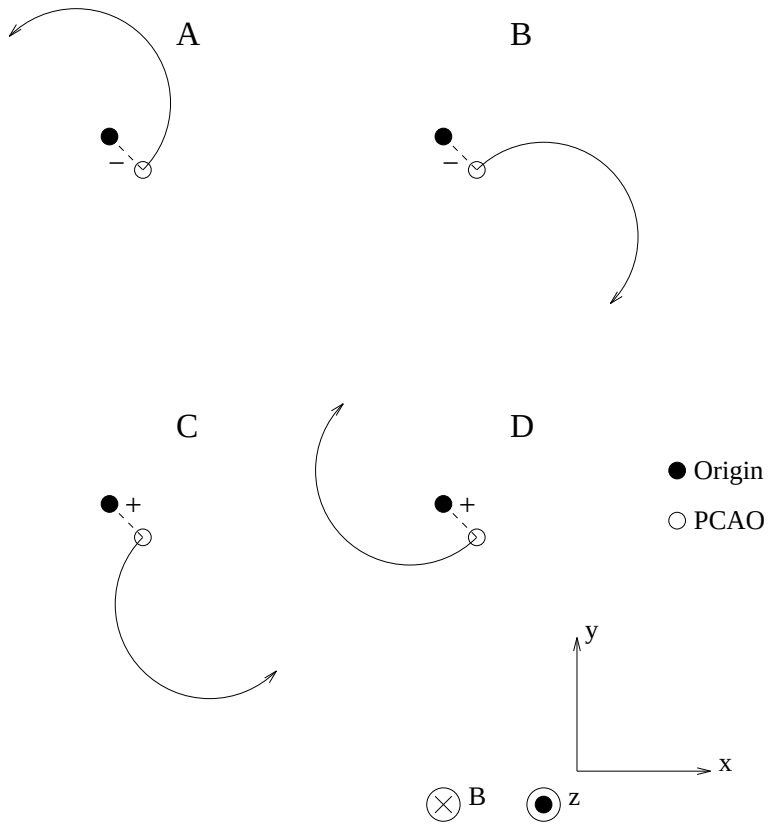

Figure 3: The sign convention for d_0.

curvature,

$$R_c = d_0 + q\rho = d_0 + \frac{1}{2\kappa},$$

and the coordinates of the center of curvature,

$$(x_c, y_c) \quad = \quad R_c(-\sin\phi_0,\ \cos\phi_0).$$

Table 2 gives the signs of q, R_c and d_0 for each part of Figure 3.

Part	q	R_c	d_0
A	$+$	$+$	$-$
B	$-$	$-$	$-$
C	$+$	$+$	$+$
D	$-$	$-$	$+$

Table 2: Signs of q, R_c and d_0 for each part of Figure 3.

Inspection of Figure 3 shows that the signed value of d_0 can be expressed as,

$$d_0 \;=\; -\mathbf{d_0} \cdot \frac{\mathbf{p_0} \times \hat{\mathbf{z}}}{|\mathbf{p_0} \times \hat{\mathbf{z}}|} = -d_{0_x} \sin\phi_0 + d_{0_y} \cos\phi_0. \tag{2}$$

Similarly, one can verify that the 2-vector $\mathbf{d_0}$ is given by,

$$(d_{0_x}, d_{0_y}) \;=\; d_0(-\sin\phi_0,\ \cos\phi_0).$$

7 Sign Convention for Drift Distances.

The following quote from Dan Peterson gives the sign convention for the distance of closest approach of a track to an axial wire: "The drift distance has the same sign as the curvature if the wire is outside the track circle. This conspires to the result that the drift distance is positive if, at the chamber layer radius, the track circle is at a larger azimuth than the wire, regardless of the charge." This reduces to the expression,

$$d_f \;=\; q\left(\sqrt{(x_c - x_W)^2 + (y_c - y_W)^2} - \rho\right). \tag{3}$$

Here (x_c, y_c) denotes the center of curvature and (x_W, y_W) denotes the position of the wire.

A similar convention applies for stereo wires. If the wire passes outside the arc of the helix, then the drift distance has the same sign as the curvature. For stereo wires Equation 3 gives the projection of the drift distance onto the r-ϕ plane; in this case (x_W, y_W) should be understood as the coordinates of the point on the wire which is closest to the track. This projection has the same sign as the full drift distance.

The signed drift distance can also be expressed in the notation of Johnson and Trilling[1],

$$d_f \;=\; -(\mathbf{P} - \mathbf{W}) \cdot \frac{\mathbf{p} \times \mathbf{w}}{|\mathbf{p} \times \mathbf{w}|}. \tag{4}$$

Here $\mathbf{W}$ is a point anywhere on the wire, $\mathbf{w}$ is a vector in the direction of the wire, $\mathbf{P}$ is a point on the track in the neighbourhood of the point of closest approach to the wire (PCAW) and $\mathbf{p}$ is the momentum vector of the track at $\mathbf{P}$. The point $\mathbf{P}$ must be sufficiently close to the PCAW that the arc from $\mathbf{P}$ to the PCAW may be adequately approximated by a straight line. This formula holds for both stereo and axial wires. Equation 2 can be considered a special case of a Equation 4. Also notice that Equation 4 has an additional minus sign relative to the sign convention used by Reference [1].

8 Sign of the Stereo Angle

Let (x_{W_0}, y_{W_0}) be the point in the plane z=0 through which the stereo wire passes and let ϕ_{W_0} be the azimuth of this point. Also let θ_s denote the stereo angle of the

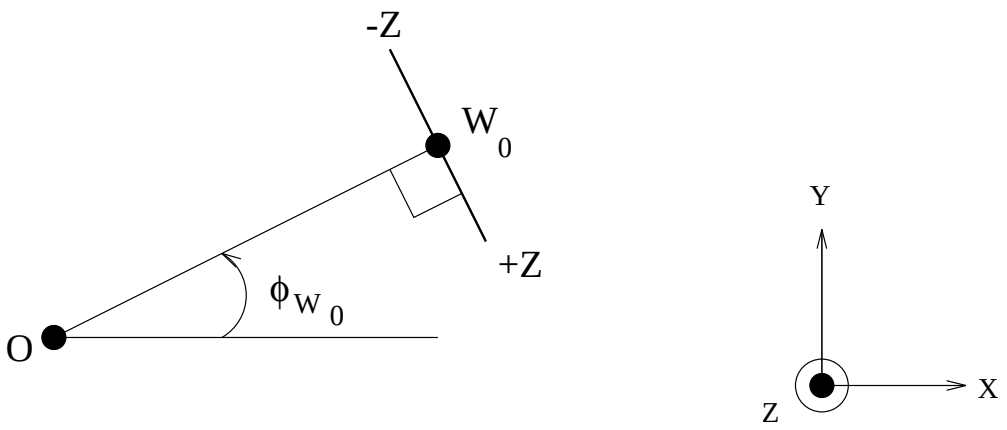

Figure 4: Projection onto the z=0 plane of a stereo wire (thick line). The thin line joins the origin (O) to the point on the wire, W_0, which lies in the plane z=0. These two lines are perpendicular to each other. For a stereo wire with positive stereo angle, the point marked $+z$ comes out of the page and the point marked $-z$ goes into the page.

wire. The projection of the stereo wire onto the plane z=0 is a line segment which is perpendicular to line segment which goes from the origin to (x_{W_0}, y_{W_0}). See Figure 4. The coordinates, (x_W, y_W), of a point on the stereo wire at a given value of z is,

$$\begin{aligned} x_W &= x_{W_0} + z \tan\theta_s \sin\phi_{W_0} \\ y_W &= y_{W_0} - z \tan\theta_s \cos\phi_{W_0}. \end{aligned}$$

Equivalently, the direction of a stereo wire is given by the vector,

$$\mathbf{w} = (\sin\theta_s \sin\phi_{W_0}, -\sin\theta_s \cos\phi_{W_0}, \cos\theta_s).$$

Figure 5 shows a view down the z-axis of DR layers 44 through 48, inclusive, in the neighbourhood of $\phi = \pi/4$. In this figure the projections of several of the stereo wires onto the z=0 plane are shown. Notice that the change in the radius of the wire between z=0 and $z = \pm z_{max}$ is small compared to the radial separation between layers.

9 Residuals

In CLEO tracking creole the two phrases "space residuals" and "time residuals" are used. The first refers to the quantity $d_m - d_f$, where d_m is the measured, signed, drift distance, computed from the measured TDC value, and where d_f was defined in section 7. The second phrase usually refers to the quantity, $|d_m| - |d_f|$, which is known as a time residual even though it has dimensions of a length. Sometimes this is reported as the equivalent time difference. More details are given in Reference [5]. One must also be careful about the sign of these two quantities: some results are presented with the sign convention opposite to that described above.

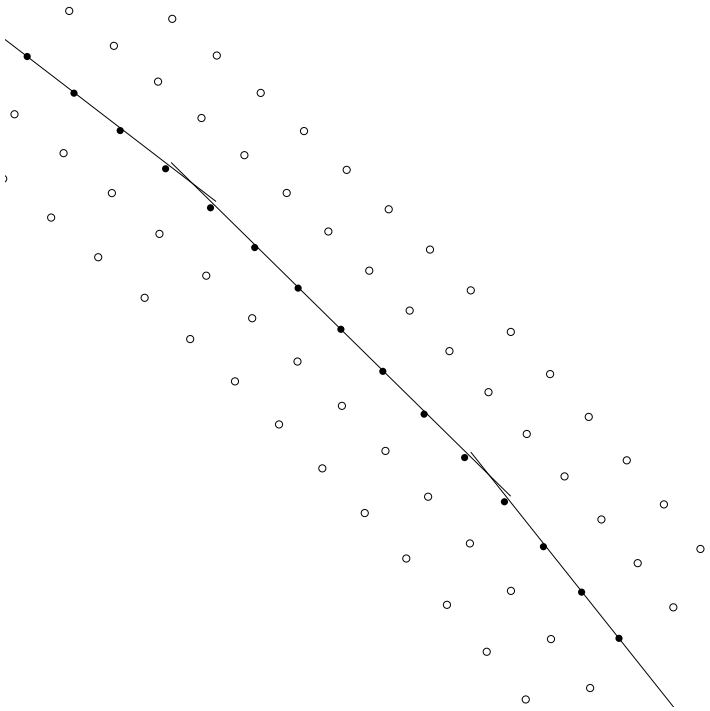

Figure 5: View down the z-axis of DR layers 44 through 48, near $\phi = \pi/4$. The positions of the sense wires in the axial layers, 44, 45, 47 and 48, are indicated by the open circles. For the stereo layer, 46, the positions of the sense wires at z=0 are indicated by the filled circles. For three of the stereo wires, the projection of the wire onto the z=0 plane is also shown (the straight lines). Counting from the lower right corner, the wires for which the projections are drawn are the first, the eighth and the last.

10 The "Cabbage" Variables

In section 2 the standard helical variables used by CLEO were described. Inside the DUET r-ϕ pattern recognition routines, however, a different set of variables are used, the "$\kappa\alpha\beta\gamma$" (pronounced Cabbage) variables. When doing the r-ϕ pattern recognition for one track, the DUET link-tree algorithm performs circle fits to many thousands of lists of hit axial layers. In this context, a list of hit axial layers includes candidate solutions to the left-right ambiguities. Because this fitter is run so frequently it must execute very quickly. In DUET, this fitter is found in the subroutines CFMTRX and CFCFIT, which implement an algorithm described in the Ph.D. thesis of Thomas Killian, a former Cornell student [2]. There is a brief description of the algorithm, and a detailed exposition of the algebra, in Reference [3]. The sign conventions used inside DUET correspond to those of Reference [3], which occasionally differ from those used in Killian's thesis.

In most tracking algorithms, a circle is described by three independent parameters

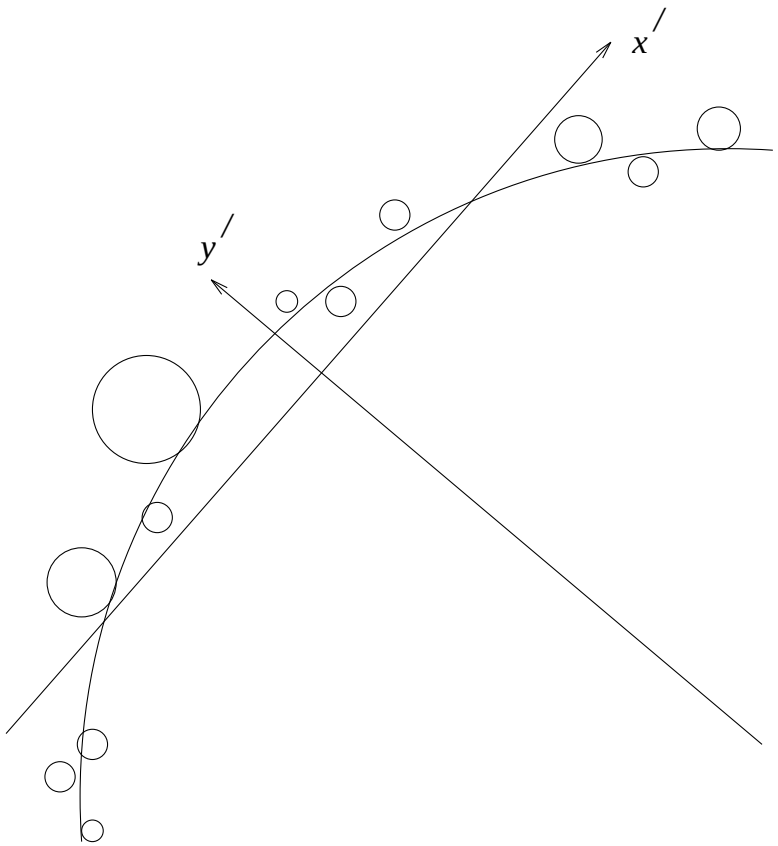

Figure 6: The coordinate system (x', y') used to define the $\kappa\alpha\beta\gamma$ variables. The large arc represents the trajectory of a particle and the small circles represent isochrones at each sense wire. The coordinate system is defined so that the weighted average values of x', y' and of $x'y'$ are all zero; the average runs over each of the hits. This figure is drawn presuming different weights at each measurement point; therefore the axes are not symmetric about the hit wires.

and the track model is non-linear in these parameters. Therefore fitting is done by linearizing the equations and iterating. In Killian's method, the track is described as a *linear* function of *four* parameters, which are related to each other by a quadratic constraint. Because this track model is linear its parameters, there is an exact solution which does not require iteration. While there is a Newton-Raphson iteration to extract one root of a fourth order polynomial, this is much quicker than an iterating a track fit. The errors made in this procedure are smallest for high momentum tracks and are reputed to remain small for most tracks found in CLEO II. The author has never carefully checked this last claim.

The essence of the method is to transform to a new coordinate system, shown in Figure 6, which is related to the lab frame by a translation, a rotation and a scale factor. Let points in the new coordinate system be denoted by (x', y'). The new coordinate system is defined such that,

$$\begin{aligned} < x' > &= < y' >= 0 \\ < x'y' > &= 0 \end{aligned}$$

$$< x'^2 + y'^2 > \quad = \quad 1,$$

where,

$$< a > \quad = \quad \frac{\sum_i a_i/\sigma_i^2}{\sum_i 1/\sigma_i^2}. \tag{5}$$

Here i runs over all of the hits on the track and σ_i is the measurement error on the drift distance for hit i. The four parameters which describe a track in this system are,

- κ the curvature. This is the same as κ in the set of helical track parameters.
- α x' of the center of curvature.
- β y' of the center of curvature.
- γ the DCAO.

The quadratic constraint is that,

$$\alpha^2 + \beta^2 - 4\kappa\gamma = 1.$$

Another quantity often used in the $\kappa\alpha\beta\gamma$ algebra is ξ, defined by,

$$\xi^2 \quad = \quad \alpha^2 + \beta^2 = 1 + 4\kappa\gamma,$$

which can be interpreted as the distance from the origin of the coordinate system to the center of curvature. As implemented in DUET, the $\kappa\alpha\beta\gamma$ algebra will work well so long as ξ can be adequately approximated as,

$$\xi \quad = \quad 1 + 2\kappa\gamma. \tag{6}$$

This restriction only applies during the link-tree portion of the DUET pattern recognition; it does not apply for the final fitter. Also, there is a second round of pattern recognition, the so called "SF" pattern recognition, which will usually find tracks which fail the link-tree algorithm due to the inadequacy of the above approximation[4].

Although the curvature in the helical system and the curvature in the $\kappa\alpha\beta\gamma$ system are the same quantity, they are carefully distinguished within DUET. The former is stored in the variables CURCF, CURCS, CURCD while the latter is stored in the variables KAPCF, KAPCS. In this note, however, they will only be distinguished when necessary.

The routines which transform between these two sets of parameters are:

CDKABG: $\kappa, \phi_0, d_0 \rightarrow \kappa, \alpha, \beta, \gamma$

CDCFID: $\kappa, \alpha, \beta, \gamma \rightarrow \kappa, \phi_0, d_0$

11 Layer Numbering Conventions

There are two layer numbering schemes used in DUET, the CD numbering scheme and the TF numbering scheme. The CD numbering scheme is the scheme used by CLEOG and by most other CLEVER processors. DUET, however, predates the CD numbering scheme,

and requires that each axial layer have a lower layer number than any stereo layer. Therefore there is a complete second copy of all of the geometry information arranged in the order required for DUET. This ordering is known as the TF ordering. The two numbering schemes are:

CD: - all anodes, starting from the innermost and working outward.

- all cathodes, starting from the innermost and working outward.

(This is the ordering used in KBITCD.)

TF: - all axial layers starting from the innermost and working outward.

- all stereo layers and cathodes, mixed together, starting from the innermost and working outward.

When the PT is replaced by the SVD, the layer numbering schemes will be,

CD: - all wire chamber anodes, starting from the innermost and working outward.

- all wire chamber cathodes, starting from the innermost and working outward.

- all Si axial layers, starting from the innermost and working outward.

- all Si z layers, starting from the innermost and working outward.

TF: - all axial layers, Si and wire chambers mixed together, starting from the innermost and working outward.

- all stereo layers, cathodes and Si z layers, mixed together, starting from the innermost and working outward.

The geometry database with arrays indexed by CD layer number is found in the sequences CDGEOMPA and CDGEOMCD, from SEQ.CMZ. These arrays are filled by routines from the library CDGEOM, either at the beginning of a CLEVER job or at the beginning of each run. There are extensive comments describing these variables in the documentation for CDGEOMCD. This documentation is not normally included when a CMZ deck is expanded into a compilable fortran subroutine. Therefore one must look in SEQ.CMZ or SEQ.CAR to find the documentation.

A duplicate geometry database, with arrays indexed by TF layer number, is found in the sequences TFGEOMPA and TFGEOMCD, from DUET.CMZ. At the beginning of each run, the TF ordering is created by the subroutines TFGMBD and TFGMIO. The TF geometry database is then filled from the CD database by the subroutines TFGMI1 and TFGMI2.

The transformation between TF and CD layers is done using the arrays:
CD to TF: ILTF = ILCDTF(ILCD)
TF to CD: ILCD = ILTFCD(ILTF),
which are found in the sequence TFGEOMCD.

12 Wire Numbering Conventions

The number of wires or cathode strips in layer ILCD is stored in NWIRCD(ILCD). Wires, or strips, are numbered 0 to NWIRCD(ILCD)-1.

Cathode layers are segmented coarsely in ϕ and finely in z. A cathode strip is identified by its layer number, its ϕ segment number (IP) and its strip number (IS). These last two can be combined to give a wire number (IW) for each cathode strip in a layer, IW=IS+IP*NWRZCD(ILCD). Here NWRZCD(ILCD) contains the number of strips in one ϕ segment of cathode layer ILCD; strips are numbered in the range 0 to NWRZCD(ILCD)-1. The ϕ segments are numbered in the range 0 to NWIRCD(ILCD)/NWRZCD(ILCD)-1.

There are several other ways in which an individual wire or strip can be identified, by (crate,slot,channel) for example. Details can be found in the CDGEOMCD documentation.

13 More Layer Numbering Conventions

Within TF3FIT, the final fitter, some additional information is encoded in the layer number. For example, hits with a negative layer number are not to be included in the fit. This is used to remove a hit with a large residual, by setting the layer number of the hit to minus itself. Also, it is sometimes interesting to look at residuals for hits which were deliberately excluded from the fit. In order to implement this, a hit with a negative layer number is added to the list. Finally, a VD wire with charge division will appear twice in the hit list. When its TDC measurement is to be included in the fit as any other axial wire, it appears in the list with its normal layer number. When its z measurement from charge division is to be used in the fit, it appears in the list with its layer number offset by QDIVAD. Currently QDIVAD=100.

14 Some Parameters of the Detectors

In the following, the phrase "the nominal radius" of a layer will be used. For an axial layer, this refers to the radius at which one would find all of the wires in a perfectly constructed and perfectly aligned chamber. For a similarly perfect stereo layer, it refers to the radius at which the wires pass through the plane z=0. This radius is stored in the variables, RTF(ILTF) and RCD(ILCD).

PT:
- 6 layers of straw tubes; $z_{end} \approx \pm 0.25m$.
- 64 tubes per layer.
- Adjacent layers are half cell staggered.
- ADC's are read out but are not used for anything.
- The chamber has a deformation called a "squash". The deformation is parameterized as follows: each wire remains at its nominal radius but is shifted in ϕ. The magnitude of the shift is sinusoidal in ϕ and the largest shift is approximately 40 μ.
- Up to run 45968, the gas was 50/50 argon/ethane at 1 atm.
- Starting at run 45969 (start of 4S4), the gas is DME, at 1 atm.
- The electron drift velocity in DME is not saturated.

VD:
- 10 anode layers; $z_{end} \approx 0.35m$.
- Inner 5 anode layers have 64 cells per layer.
- Outer 5 anode layers have 96 cells per layer.

- Adjacent layers within each group of 5 are half cell staggered.
- Field wires on the layer 5/layer 6 boundary are correct for layer 6. Hence layer 5 has a more distorted field cage than does layer 6.
- Inner cathode: 64 segments in z and 8 segments in ϕ (pitch 5.85 mm). Here pitch refers to the distance in z between the centers of adjacent strips.
- Outer cathode: 96 segments in z and 8 segments in ϕ (pitch 6.95 mm)
- Both ends are instrumented with both ADC's and TDC's.
- ADC's are used to get z from charge division but are not used to for dE/dx measurements.
- Gas is 50/50 argon/ethane at 20 PSIA, (1.38 atm.).

DR:
- 51 anode layers; $z_{end} \approx 0.95m$.
- Pattern of layers: $10 \times [aaas] + aaaaa + s + aaaaa$, where a represents an axial layer and s a stereo layer.
- Within one $[aaas]$ multiplet, each axial layer has the same number of cells. Each multiplet is said to have have layers with big, small, and medium sized cells.
- Within one $[aaaaa]$ multiplet, each layer has the same number of cells.
- All stereo layers have a different number of cells than either of the adjacent axial layers.
- At axial/stereo boundaries the field wire configuration is correct for the axial layers.
- Adjacent layers within each group of axial layers are half cell staggered.
- Inner cathode: 96 segments in z and 16 segments in ϕ (pitch 10.0 mm).
- Outer cathode: 192 segments in z and 8 segments in ϕ (pitch 9.51 mm).
- Each wire is instrumented, at one end only, with a TDC and an ADC.
- Each cathodes strip is also instrumented with both a TDC and an ADC.
- Gas is 50/50 argon/ethane, at 1 atm.

Notice that, for both the VD and the DR, the inner cathode strips do not cover the full z extent of the chamber. They only extend far enough in z that, for tracks from the neighbourhood of the interaction point, they do not reduce the solid angle acceptance of the detector.

Tables 3 and 4 give some more device parameters

15 Effective Radius of the Cathodes

The pulses on the cathodes are the image of the charge produced at the neighbouring anode during gas amplification. Therefore the z measurement made by a cluster of cathode strips is a measurement of the z at which the gas amplification took place. In other words, an outer (inner) cathode, measures the z at which the track crossed a cylinder with a radius just larger (smaller) than radius of the neighbouring anode wire. This radius is known as the effective radius of the cathode. The variable `RTF(ILTF)` contains this effective cathode radius, but the variable `RCD(ILCD)` contains the radius at which the cathode strips are located. The variable `REFFCD(ILCD)` contains the displacement of the effective cathode radius from the radius of the neighbouring anode.

ILCD	ILTF	Device	NWIRCD	RCD(mm)	TANSCD	PHIFCD(rad)
1	1	PT	64	47.264	0.00000000	3.14988899
2	2	PT	64	51.453	0.00000000	3.10080147
3	3	PT	64	56.022	0.00000000	3.14988899
4	4	PT	64	60.996	0.00000000	3.10080147
5	5	PT	64	66.411	0.00000000	3.14988899
6	6	PT	64	72.306	0.00000000	3.10080147
7	7	VA	64	84.727	0.00000000	3.14154887
8	8	VA	64	92.247	0.00000000	3.09246135
9	9	VA	64	100.434	0.00000000	3.14154887
10	10	VA	64	109.348	0.00000000	3.09246135
11	11	VA	64	119.053	0.00000000	3.14154887
12	12	VA	96	127.795	0.00000000	3.14122152
13	13	VA	96	135.249	0.00000000	3.10849667
14	14	VA	96	143.137	0.00000000	3.14122152
15	15	VA	96	151.485	0.00000000	3.10849667
16	16	VA	96	160.320	0.00000000	3.14122152
17	17	DA	96	198.994	0.00000000	-0.41895592
18	18	DA	96	213.041	0.00000000	-0.25533128
19	19	DA	96	227.088	0.00000000	0.10464300
20	60	DA	108	240.063	0.03355476	-0.37532270
21	20	DA	120	255.182	0.00000000	-0.23569635
22	21	DA	120	269.229	0.00000000	-0.26187629
23	22	DA	120	283.276	0.00000000	-0.65457541
24	61	DA	132	296.213	-0.03758329	-0.13335660
25	23	DA	144	311.370	0.00000000	-0.41895592
26	24	DA	144	325.417	0.00000000	-0.22260639
27	25	DA	144	339.464	0.00000000	0.10464294
28	62	DA	156	352.339	0.04155730	-0.34847149
29	26	DA	168	367.558	0.00000000	-0.36285609
30	27	DA	168	381.605	0.00000000	-0.23195639
31	28	DA	168	395.652	0.00000000	-0.66205543
32	63	DA	180	408.809	-0.04170920	-0.13097663

Table 3: Properties of the first 32 CD layers in the PT/VD/DR configuration. The columns give the CD layer number, the TF layer number, the device name, the number of wires in the layer, the nominal radius of the layer, the tangent of the stereo angle and the ϕ of the first wire in the layer. The less obvious device name mnemonics are VA=VD anode, DA=DR anode, VC=CD cathode and DC=DR cathode. See section 15 for a more complete explanation of `RCD` for cathode layers. Also note that the stereo angles given in the CLEO II NIM article [14] are incorrect. The ones given in this table are correct.

ILCD	ILTF	Device	NWIRCD	RCD (mm)	TANSCD	PHIFCD (rad)
33	29	DA	192	423.746	0.00000000	-0.38623103
34	30	DA	192	437.794	0.00000000	-0.27169380
35	31	DA	192	451.841	0.00000000	0.13736780
36	64	DA	204	464.896	0.04561331	-0.31115621
37	32	DA	216	479.935	0.00000000	-0.31714511
38	33	DA	216	493.982	0.00000000	-0.24442303
39	34	DA	216	508.029	0.00000000	-0.54985565
40	65	DA	228	520.979	-0.04950263	-0.10893032
41	35	DA	240	536.123	0.00000000	-0.20951647
42	36	DA	240	550.170	0.00000000	-0.19642650
43	37	DA	240	564.217	0.00000000	-0.41895598
44	66	DA	252	577.363	0.04957073	-0.28805625
45	38	DA	264	592.311	0.00000000	-0.28805628
46	39	DA	264	606.358	0.00000000	-0.20475647
47	40	DA	264	620.405	0.00000000	-0.47845584
48	67	DA	276	633.436	-0.05343856	-0.11162622
49	41	DA	288	648.499	0.00000000	-0.41895598
50	42	DA	288	662.546	0.00000000	-0.27714798
51	43	DA	288	676.594	0.00000000	-0.41895598
52	68	DA	300	689.508	0.05730266	-0.26711234
53	44	DA	312	704.688	0.00000000	-0.26791787
54	45	DA	312	718.735	0.00000000	-0.19743343
55	46	DA	312	732.782	0.00000000	-0.34847152
56	69	DA	324	745.852	-0.05734350	-0.15230846
57	47	DA	336	760.876	0.00000000	-0.38155609
58	48	DA	336	774.923	0.00000000	-0.22260645
59	49	DA	336	788.970	0.00000000	-0.23195642
60	50	DA	336	803.017	0.00000000	-0.07300676
61	51	DA	336	817.064	0.00000000	-0.23195642
62	70	DA	360	830.084	0.06122083	-0.28805628
63	52	DA	384	845.158	0.00000000	-0.01807564
64	53	DA	384	859.205	0.00000000	-0.66439295
65	54	DA	384	873.252	0.00000000	-0.54167449
66	55	DA	384	887.299	0.00000000	-0.40259355
67	56	DA	384	901.346	0.00000000	-0.21442522
68	57	VC	512	82.000	0.00000000	3.49497795
69	58	VC	768	166.000	0.00000000	3.48025179
70	59	DC	1536	191.977	0.00000000	0.20281753
71	71	DC	1536	908.377	0.00000000	0.39916706

Table 4: Properties of CD layers 33 through 71 in the PT/VD/DR configuration. See the caption of Table 3 for a description of the table.

```
      ILCD = ILTFCD(ILTF)
      ZZ   = ZW - XXOTF(3,ILTF)
      PHIW = PHIFCD(ILCD) + IW*CELLCD(ILCD) + DUSQSH(ILCD,IW)
      XWO  = RTF(ILYR)*COS(PHIW) + XXOTF(1,ILYR) +
     +       ZZ * UUOTF(1,ILYR)
      YWO  = RTF(ILYR)*SIN(PHIW) + XXOTF(2,ILYR) +
     +       ZZ*UUOTF(2,ILYR) -
     +       BSAGCD(ILCD)*(1. - (ZW/ZENDTF(ILTF))**2)
      RWO  = SQRT ( XWO**2 + YWO**2 )
      XW   = XWO + ZZ * TANSTF(ILTF) * YWO/RWO
      YW   = YWO - ZZ * TANSTF(ILTF) * XWO/RWO
```

Figure 7: Code fragment which illustrates the use of the alignment parameters.

16 Alignment Parameters

The misalignment of detector components is accounted for by the following algorithm, which is coded in the subroutine CDCORF. Consider a wire with TF layer number ILTF and wire number IW. The point, XW, YW, at which this wire intercepts the plane $z =$ ZW is given by the code fragment shown in Figure 7. The variables referenced in this code fragment are:

XXOTF The displacement vector of the center of the layer from its nominal position.

PHIFCD The azimuth of wire zero.

CELLCD The width of a cell, in radians.

DUSQSH A function which returns the "squash" deformation of the PT.

RTF The nominal radius of the layer.

UUOTF The "tilt" parameters of the layer.

BSAGCD The magnitude of the wire sag, due to gravity, at the midpoint of the wire.

ZENDTF The value of $|z|$ at the ends of the chamber.

TANSTF Tangent of the stereo angle.

The essence of the algorithm can be summarized as follows: the wire direction is assumed to be unchanged either by misalignment or by gravity. These effects are accounted for by fudging the point in the z=0 plane through which the wire passes, (XWO,YWO). This "effective point in the z=0 plane" is, therefore, dependent on the value of z at which the track passes closest to the wire.

Two other approximations are made in the treatment of chamber tilts. Firstly, the tilt corrections are only performed once, at the start of the fit, using track parameters from the pattern recognition. Secondly, the value of z used to correct for the tilts is not the value of z at the point on the wire which is closest to the track. Rather it is

the value of z at which track crosses the nominal radius of the layer. In practice the tilts are small enough that neither of these should be a serious problem. It may be possible, however, to see the effects of the former in the PT: if a cathode is deleted during the final fitter, then one can imagine that the z position near a PT layer might change by as much as 1 cm. This would result in a shift of the effective wire position at z=0 by about half of the resolution of the PT.

Another quirk of the above algorithm is that the stereo wires are assumed to be perpendicular to the line from the origin to `(XWO,YWO,0.0)`, not perpendicular to the line which runs along the azimuth `PHIW`. In practice the tilt parameters for the stereo wires are zero and the offsets (`XXOTF`) are of the order of tens of microns. Therefore, the difference between these two understandings of the alignment of the stereo wires is negligible.

17 Nominal Resolutions

Figure 8 shows the resolution functions used by `TF3FIT` for each of the tracking devices. Although these resolution functions depend on many parameters, each resolution function is parameterized only as a function of its most important parameter. For anodes that parameter is the normalized drift distance, d/d_{max}, and for the cathodes it is $|\cot\theta|$. For several of the devices, different resolution functions have been used during the compress of different data sets and Figure 8 shows all of these. These resolution functions are stored as `DATA` statements in the routine `WGTDCD` from the library `CDOFFCAL`. For the innermost and outermost axial layers of the DR, the resolution function used by `TF3FIT` is two times poorer than that shown.

The nominal granularity of the TDC's is approximately 4 counts per ns. For the VD and DR, in which the nominal drift velocity is in the neighbourhood of 50μ/ns, this corresponds to approximately 12.5μ per TDC count. At the pressure and electric field in a PT cell, the drift velocity in DME is not saturated. Therefore the drift velocity is slower and one TDC count corresponds to a drift distance of more than 12.5μ.

18 The Entrance Angle

Because the drift cells in the DR and VD are not circular, the isochrones are also not circular. The correction for non-circular isochrones is expressed in terms of a parameter known as the entrance angle, θ_e Actually the parameter is the sine of this angle, defined as follows. First, find the point at which the track crosses the cylinder, centered at the origin, that has the nominal radius of the wire layer. Next define two unit 2-vectors, the vector from the origin to the intersection point, $\hat{\mathbf{r}}$, and the $\hat{\mathbf{p}}_\perp$ of the track at the intersection point. Now, let (x, y) denote the intersection point, and let $R^2 = x^2 + y^2$. In this notation,

$$\hat{\mathbf{r}} = (x, y)/R \qquad \hat{\mathbf{p}}_\perp = q(-(y - y_c), (x - x_c))/\rho.$$

Some algebra gives,

$$\sin\theta_e \;=\; -(\hat{\mathbf{p}}_\perp \times \hat{\mathbf{r}})_z$$

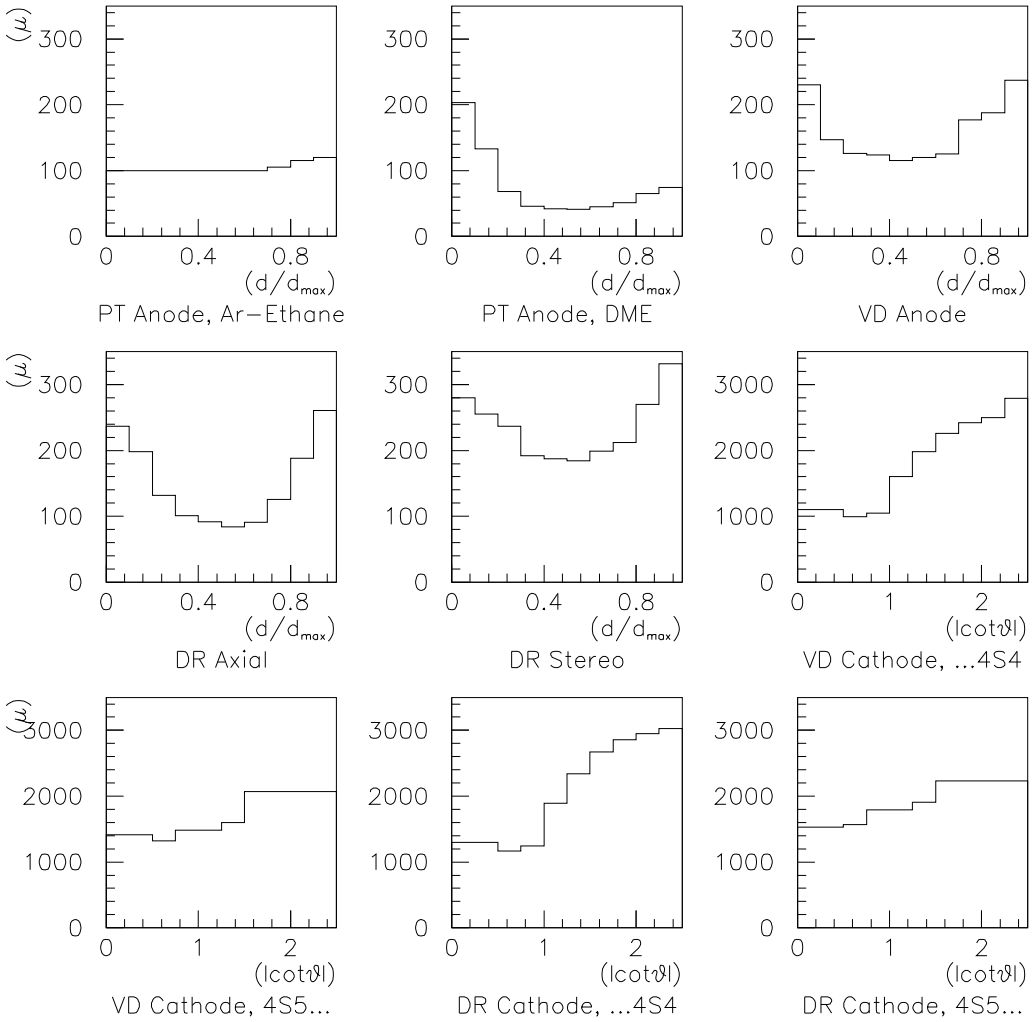

Figure 8: The resolution used in `TF3FIT`, in μ, for each of the tracking devices. For each hit, the resolution is linearly interpolated using the data in the above histograms.

$$= \quad (\kappa R^2 - \gamma)/R.$$

The angle θ_e is known as the entrance angle because, for a sufficiently straight track, it is the angle away from the radial direction with which the track enters the cell. Note that the sign convention above is that found in the code; it is the opposite of that described in reference [3].

Clearly this formulation ignores chamber misalignment. Also, even for a perfectly aligned chamber, the entrance angle is probably not the optimal parameter with which to parameterize this correction. Both of these approximations are believed to be adequate but they author has not carefully checked either of them.

19 PT Pairwise Requirement

The following requirement on PT hits was empirically found to improve the resolution on the impact parameter for Bhabha and μ pair events. It is therefore included under

normal operation of DUET. The requirement is: a PT hit will be included on the track only if a hit from at least one of its neighbouring layers is also included on the track. The reasoning behind this has to do with the half cell stagger between layers in the the PT. If hits from two adjacent layers are included on the track then the resolution of the sign ambiguity is straightforward. If a hit is included when neither neighbour is present, then the probability of incorrectly solving the sign ambiguity is increased. It was decided that simply dropping such hits is better than including some fraction of them with the wrong solution to the sign ambiguity.

Because layers 1 and 6 have only one neighbour, this requirement reduces their efficiency compared to that of the other four layers of the PT. Here "efficiency" refers the number of times that a layer was included in the final fit divided by the number of tracks which traversed that layer.

In the 4S9 running period several sectors of the PT could not hold voltage. People worried that the combination of dead sectors and the pairwise requirement might unacceptably lower the efficiency of the PT. For this reason the pairwise requirement was modified so that a wire will also be included in the fit if either of its neighbours is a known dead wire. At this writing the effect of this change is still being evaluated.

20 VD East

The VD is instrumented with ADC's and TDC's at both ends of each wire and both sets of data are read into the data stream. In order to distinguish the information from the two ends of the wire, the following convention is used. Consider one of the inner 5 layers, with 64 wires per layer. The measurements from the west end have wire numbers 0-63 while those from the east end have wire numbers 64-127. For this layer the variable NWIRTF(ILTF), the number of wires in the layer, will have a value of 64 (not 128). Therefore one sometimes sees the following construction,

```
IF (  IWIR .LT. NWIRTF(ILTF) ) THEN
   do something for west end
ELSE
   do something similar for the east end
ENDIF
```

Until the start of the 4S9 data taking period the timing information on the east end was read out but was ignored during pass2. At that time the VD east data boards were modified so that they should be superior to the VD west data boards. The modification was to change some resistors in the circuits which charge and discharge the timing capacitor. The net result is that, after a beam crossing which generates a VD hit but no trigger, the capacitor recovers more quickly to its quiescent state. Therefore fewer VD east timing capacitors than before should be contaminated by data from previous beam crossings.

When DUET was modified to use VD East hits, the following changes were made. The variable LUSVDE was added to the control common block and to the namelist file. When LUSVDE=.TRUE., DUET uses the east hits from the VD and, when it is .FALSE.,

DUET uses the west hits. In order to implement this, the subroutine CDRWCP swaps the wire numbers of east and west hits; that is, the east wires are shifted into the range 0 to NWIRCD(ILCD)-1 while the west wire are shifted into the range NWIRCD(ILCD) to 2.*NWIRCD(ILCD)-1. DUET then proceeds as normal, using the hits with wire numbers less than NWIRCD(ILCD). When it comes time to make corrections for such things as the signal propagation, the code checks LUSVDE to determine how to perform the correction.

21 The Stale Data Bit

The VD data boards have electronics which can detect the following condition: a wire was hit in a previous beam crossing, for which there was no trigger, but there was no hit on that same wire in the current beam crossing, for which there is a trigger. Because the data boards do not have fast reset circuitry, the recovery time of the TDC capacitor is many beam crossings and the above circumstance may generate a hit which looks like an in-time hit. Such a hit is known as a stale hit. In order to flag stale hits, a bit is set in the west end TDC word for that wire. The east end data boards do not have the electronics to detect stale data. Stale hits are readout by the DAQ system and are in the event record. They can be recognized by the presence of the "stale data bit" in the west TDC value: any west wire with a TDC value greater than 4095 is stale. During the history of CLEO this bit has moved around within the west end TDC word but a test of greater than 4095 is correct for all time periods.

Careful reading of the above definition will show that the following holds: the stale data bit is only useful to flag wires which were not hit in the current event; if a wire is hit in the current event there is no way to tell if the TDC reading was corrupted by a previous beam crossing.

The modification to the VD east data boards, mentioned in the section 20, was to shorten the recovery time of the TDC capacitors. With this modification, the number of hits corrupted by previous beam crossings should be smaller in the east end data than it is in the west end data.

References

[1] A. D. Johnson and G. H. Trilling, "Orbit Reconstruction Program for SPEAR Mark II Detector: ARCS", 1978. This is available as an appendix to A. Weinstein, "A Collection of Formulas Useful in Particle Tracking", SDC Detector Note SDC-90-00076, 1990.

[2] T. Killian, "Analysis of the Four Pion Exclusive Channel in Inelastic Electron-Proton Scattering", Ph.D. Thesis, Cornell University, 1978, pp. 30-37.

[3] D. G. Cassel and M. Ogg, "DUET — a Track-Finding Program for Cylindrical Geometries", CSN 83/333.

[4] R. Kutschke, "DUET Flow Control", CSN 94/335.

[5] A. Bellerive, S. Jones, M. Garcia-Sciveres "Off-line Calibration of the CLEO II Drift Chambers", CBX 94-39.

[6] P. Avery, "The Charged Particle Energy Loss Correction in CLEO", CBX 92-40.

[7] P. Avery, "Applied Fitting Theory I: General Least Squares Theory", CBX 91-72.

[8] P. Avery, "Applied Fitting Theory II: Determining Systematic Effects by Fitting", CBX 91-73.

[9] P. Avery, "Applied Fitting Theory III: Non-Optimal Least Squares Fitting and Multiple Scattering", CBX-91-74.

[10] P. Avery, "Applied Fitting Theory IV: Formulas for Track Fitting", CBX 92-45.

[11] P. Avery, "Applied Fitting Theory V: Track Fitting Using the Kalman Filter", CBX 92-39.

[12] C. D. Jones and N. Katayama, "SVD Numbering Scheme for all Elements", CBX 93-06.

[13] T. Nelson, H. Nelson and J. Gronberg, "Geometry of the Silicon Vertex Detector", CBX 93-72.

[14] Y. Kubota et. al., Nucl. Inst. Meth. **A320** (1992) 66.